Non-uniformity correction in a Long Wave Infrared Focal Plane Array as a calibration temperature function

Augusto Cezar Gomes Santos[1], Gustavo Soares Vieira [1], and Ruy Morgado Castro[2]

[1]Divisao de Física Aplicada; Instituto de Estudos Avançados (IEAv/CTA); São José dos Campos – SP, Brazil
[2] Divisão de C4ISR; Instituto de Estudos Avançados (IEAv/CTA); São José dos Campos – SP, Brazil.
e-mail: augusto.cezar@eb.mil.br

***Abstract*— Despite the manufactory process, all detector or pixel in a Focal Plane Array (FPA) has a different responsivity and off-set when evaluated. These variations result in a specific kind of noise, called Fixed Pattern Noise (FPN) or spatial noise. During the image processing, pixels that have a large deviation in responsivity or in their noise are considered bad pixels, and have their influence removed during the exhibition of a scene. Knowing the response of all pixels to a uniform irradiation is the first test procedure in an FPA characterization. However, during the Non-uniformity correction and bad pixel replacement it is necessary to choose two reference temperatures, calibration points, and these temperatures affect important parameters such as Uniformity, Noise Equivalent Temperature Difference (NETD) and Signal Transfer Function (SiTF). Following standard characterization methods, this work presents a study of the calibration temperatures influence on the Non-Uniformity Correction (NUC) quality by comparing uniformity, bad pixel number, NETD and SiTF values during characterizations.**

***Index Terms*— Focal Plane Array; Long Wave Infrared; Noise Equivalent Temperature Difference; Signal Transfer Function; Uniformity.**

I. Introduction

A Long Wave Infrared Focal-Plane Array (LWIR FPA), is an infrared image device consisting in an array of sensing pixels placed in the focal plane of an optical system. With a spectral response from 8μ to 14μm, they can be considered the most important thermal imagers module when used for thermal imaging purposes. Knowledge of precise LWIR FPA sensor parameters is needed because these determines the thermal imagers performance limits.

For an FPA test, usually it is necessary to evaluate response, noise, and image resolution (geometrical and spectral) parameters [1], [2]. Here, the setup is intended only for the first two parameters.

Response parameters give us information about system response to targets of different temperatures, emissivity or sizes. The main test for this parameter, when the goal is to generate a temperature map, is the response function, that is an output signal function versus target temperature (absolute or relative). From it, three digital parameters can be extracted: Signal Transfer Function (SiTF), saturation level, and dynamic range [3], [4].

Noise parameters are also important and the Noise Equivalent Temperature Difference (NETD) will be used to characterize the calibration points in the noise parameters classification. The NETD is a laboratory measure that can be specified as a minimum temperature difference value that can be observed in all detector channels or as a channel average [5], [6].

All parameters together with bad pixel and uniformity analysis will be used to evaluate the best calibration temperature pair during non-uniformity correction process.

II. LWIR FPA Tests

A. Calibration and NUC Process

Once the FPA reading is being performed, a raw image of the sensors is displayed. Such an image, as shown in Fig. 1, will exhibit defects and excessive noise, and will require post-processing techniques to eliminate this undesirable problem.

For FPAs, the main noise in a raw picture is called Fixed Pattern Noise (FPN). This noise happens because each element on the FPA has different response for the same received stimulus. Its main feature is the display of noisy tracks.

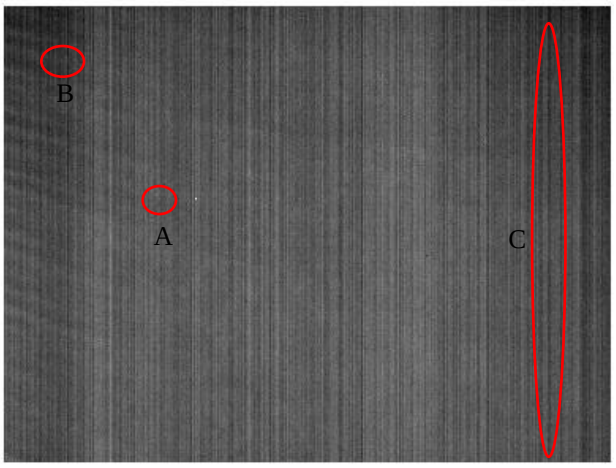

Fig. 1 – Defects in a raw image. In A, a dead pixel, B a low frequency non uniformity and in C a non-uniformity in column

Many studies and techniques to eliminate FPN have been made and the non-uniformity correction technique (NUC) has been created. In this case, the matrix is subjected to uniform and constant radiation and the response given by each sensor is adjusted [1], [7], [8]. Doing this, each pixel in the matrix is separately analyzed. The response taken as linear in the temperature interval and the angular and linear coefficients are adjusted in order to eliminate the FPN. In Fig. 2 (a) the response of three different pixels of a matrix is schematically shown, presenting a different behavior each. The process of standardizing the response matrix begins by standardizing at a point called the calibration point (b). From this, the angular coefficient adjustment of the pixel responses is performed (c), and finally the linear coefficient adjustment (d).

Digital Object Identifier 10.29292/jics.v14i3.64

Since each sensor element has a characteristic equation, it will have a specific ordered pair (a, b), (1), responsible for determining the sensor response equation. For adjusting different response line equation, a specific ordered pair (α, β), (2), is then required. So, these ordered pairs will be responsible for the image uniformity.

$$R_{m,n(raw)} = a_{m,n} \cdot \phi + b_{m,n} \quad (1)$$

$$R_{m,n(adj.)} = \alpha_{m,n} \cdot a_{m,n} \cdot \phi + b_{m,n} + \beta_{m,n} \quad (2)$$

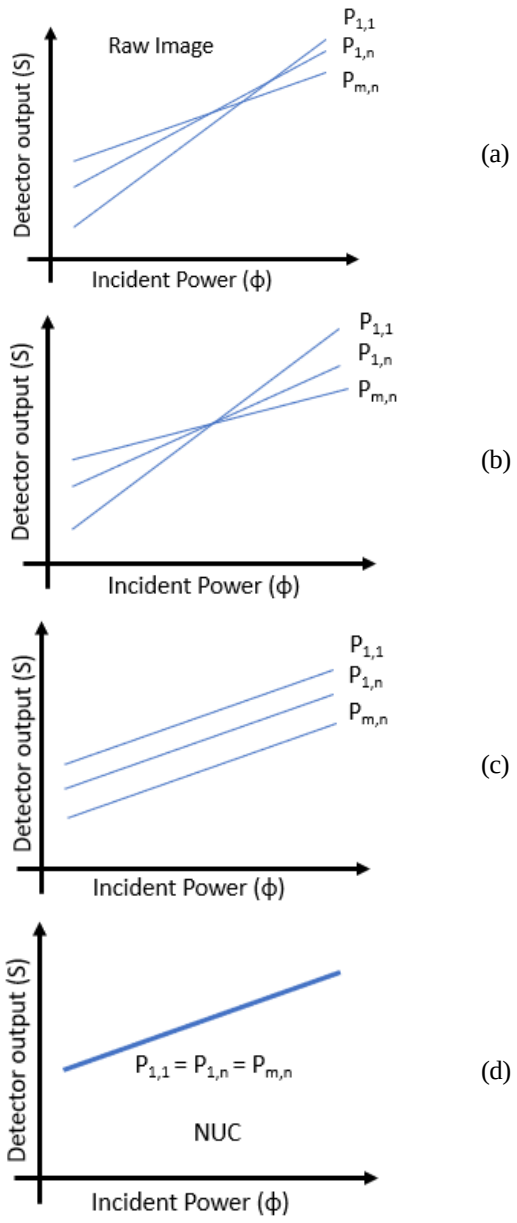

Fig. 2 - Mathematical process for FPA detectors non-uniformity correction.

The next step in the post processing image is the bad pixel determination and location.

B. Mapping bad pixels

Such a large number of pixel in an FPA will inevitably contain pixels that do not meet certain quality requirements. In fact, the number of bad pixels is an important parameter in quality and it is responsible for some company's classification. There is not a unique definition of what is considered a bad pixel. There is no standardization, each author or manufacturer uses a specific one for their application.

Normally, it is possible to define three types of defects in the pixel, they are:

1. Dead pixels: pixels that always produce the same signal;
2. Noisy pixels: pixels that have noise greater than a fixed limit, and
3. Flashing or floating pixels: pixels with temporal behavior clearly different from the considered as good pixels.

However, this classification is not universal and strongly depends on the context. In a simplified way, the bad pixel is all that behaves differently from the others when subjected to the same stimulus. Thus, to characterize a normal pixel, a comparative analysis between the pixels must provide a parameter for each pixel describing how it is good or bad. The comparison should be made when the detector set is looking at a uniform and stable scene, which produces a constant temporal and spatial optical signal for each pixel and taking a series of frames from the detector set [9], [10].

C. Uniformity

Uniformity is a parameter that determines spatial noise caused by the signal variation in columns and rows no matter which frame has been analyzed. These parameter is part of the 3D noise model being the component σVH [1], [3], [4]. An alternative used by large characterization companies defines uniformity as a dispersion measure of maximum and minimum values in a frame.

$$U = 100\,x\left[1 - \frac{V_{max} - V_{min}}{V_{max} + V_{min}}\right] (\%) \quad (3)$$

D. Response parameters

Signal Transfer function, SiTF, or the responsivity is the linear part of the response function. It is calculated as the tangent angle between linear part of the responsivity function and the temperature axis (the slope of the linear part) [3], [4]. It is important to note that the response is taken as a function of a target temperature, not as function of incident power, as illustrated in Fig. 2. It is an important source of nonlinearity in the curve. Saturation level is the upper part of the responsivity function, and dynamic range is the ratio between maximum and minimum measurable input signal.

When performing SiTF test, it is necessary to fit a least-squares regression to the data set. It will provide the best estimate for SiTF [2].

$$SiTF = \frac{N\sum_{i=1}^{N}\Delta V_i \Delta T_i - \sum_{i=1}^{N}\Delta V_i \sum_{i=1}^{N}\Delta T_i}{N\sum_{i=1}^{N}(\Delta T_i)^2 - \left(\sum_{i=1}^{N}\Delta T_i\right)^2} \quad (4)$$

The value of offset can be done using the relationship.

$$V_{OFFSET} = \Delta V_{AVE} - SiTF\ \Delta T_{AVE} \quad (5)$$

As it has been shown, $SiTF_{AVE}$ is a statistical parameter and has to be calculate as follow:

$$SiTF_{AVE} = \frac{\sum_{i=1}^{N} SiTF_i}{N} \quad (6)$$

$$\sigma_{SiTF}^2 = \frac{N\sum_{i=1}^{N}(SiTF_i)^2 - \left(\sum_{i=1}^{N} SiTF_i\right)^2}{N(N-1)} \quad (7)$$

E. Noise parameters

Technical data offered by manufacturers of most LWIR FPA will show a parameter called "thermal sensitivity", "thermal resolution", "temperature resolution" or "NETD" that provide information about the FPA noise. The parameter mentioned above has different names but usually means Noise Equivalent Temperature Difference (NETD), but different definitions and different measurement techniques of NETD are used in literature [1], [5].

According to its classical definition, NETD is defined as the blackbody temperature difference between a target and its background required to produce a signal-to-noise (rms) ratio of unity at a suitable point in the output electrical channel. Although the definition does not state it clearly, NETD is a metric of only high frequency temporal noise along the video line.

So, the NETD is the temperature difference required to achieve a signal to noise ratio of unity and it is an excellent diagnostic indicator of system sensitivity because it verifies optimum system performance being on a practical point of view, the minimum signal step that can be recognized by the system [11],[12], [13].

$$NETD = \frac{V_{RMS}}{\Delta V} x \Delta T \quad (8)$$

Where:

V_{RMS} - V (RMS) of random noise expressed in Volts.

ΔV - Signal of the system expressed in Volts

ΔT - Temperature difference (Blackbody).

III. Methods and Discussion

A. Test Set

In order to characterize the device under test (DUT), and compare with the information regarding the characteristics of the FPA, the present work used the automated system FPA tests, PI-7700 from the american company Pulse Instrument. This apparatus, from now on called PI-7700, is composed of controlled voltage sources, clock drivers, amplifiers, and specific software for FPA reading and test routine.

Using PI-7700, it was possible to read data direct from the FPAs Read-Out Integrated Circuit (ROIC), without any interaction between FPA and a camera or camera core.

For the electro-optical tests, it was also used a large blackbody of the israeli company CI-Systems. The blackbody, model SR800, of 12 inches and emissivity of 0.97 was used as the standard source of radiation, able to uniformly irradiate all pixels at the FPA.

An aluminum target with a central circle, 10 cm in diameter, was made and an ethyl vinyl acetate plate was glued onto the front surface of this target to avoid reflections of radiation on the surface of the sensor, as well as the back surface was kept in metal, in order to reflect the rays coming from the blackbody, Fig. 3.

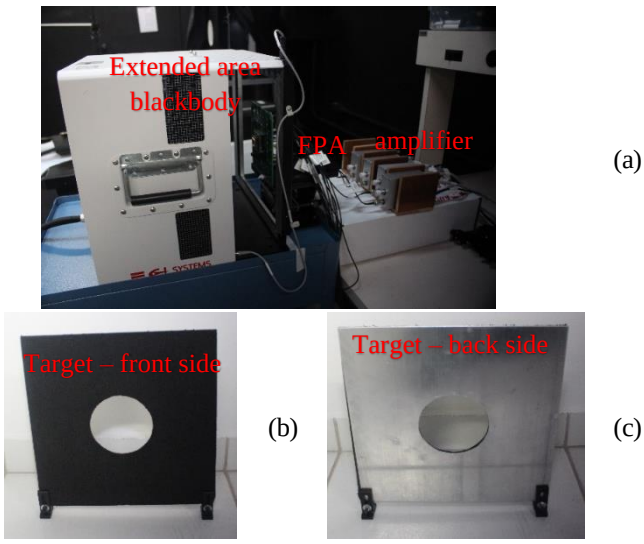

Fig. 3 – Test Setup, in (a) the FPA in front of the blackbody and the circular target, in (b) and (c) the aluminum target to keep f/1.4

All procedure done in this work have followed the same step sequence:

1. Set the FPA, with a fixed value of Gain (GFID), integration time, blind detector bias (VSK), FPA temperature stability and laboratory climatic condition (relative humidity – RH and temperature - T) as illustrated in Table 1. Changing that parameters will imply in a different FPA responsivity [14],[15].

Table 1 - Parameters used for the FPA.

Parameter	Value	Parameter	Value
FPA Size:	392 x 296	f/#:	1.4
GFID (V):	3.2	D (mm):	14
VSK (V):	5.404	T (°C):	20 ± 2
Integration Time (µs)	69	RH (%):	48

2. Use an extended area blackbody to illuminate all pixels of the FPA UL03 26 2 (392 x 296 pixel) at two known temperatures;

a. Change the lower temperature, TCold, and the higher temperature, THot in 5 °C steps, (15 °C, 20 °C until reach 65 °C).

3. Record a few frames to evaluate the average and calculate the deviation in response of all pixels;

a. Calculate the bad pixel in "cold frame", TCold, i.e., the lower temperature of pair;

b. Calculate the bad pixel in "hot frame", THot, higher temperature of pair;

c. Calculate the bad pixel in difference between hot and cold frame;

In this step it was necessary an adaption in a detector company test procedure [15]. While the company has used 20% in sensitivity and 50% in NETD error, in this work, a pixel was

considered bad if any of the following conditions were met.
i. The operating point is outside of the previously defined voltage range of the offset value dispersion.
ii. The sensitivity differs more than ±3 standard deviation from the mean value [3].

4. Count all pixels out of the predetermined interval.

5. A representative way to express a calibration point set is CxxHyy, which means cold temperature was xx and hot temperature was yy.

The macro-steps of the development of this work were:
a) reading the FPA and extracting some images without optic coupling, only using the circular target;
b) determining the FPA responsivity;
c) analyzing pixel response, checking pixels that do not meet the specification, and classifying them as a bad pixel;
d) doing NUC process, removing fixed pattern noise; and
e) studying the influence of reference temperature variation in the non-uniformity correction.

For some steps, SiTF, NETD, uniformity and operability were used in order to verify the data collected.

B. Calibration and bad pixel analysis

Three standard deviation definition causes a large number of pixels to be considered defective. However, in percentage, bad pixel number was always less than 1.5%. Assuring an operability greater than 98.5%. It is actually expected, due to the statistical criterion.

It was not possible to infer, apparently, the relation between the choice of reference temperatures and bad pixel quantity. Even when performing a basic statistics analysis, mean and standard deviation as a function of temperature, shown in Fig. 4, it was possible to observe any trend in relation to the number of defective pixel and the choice of the reference.

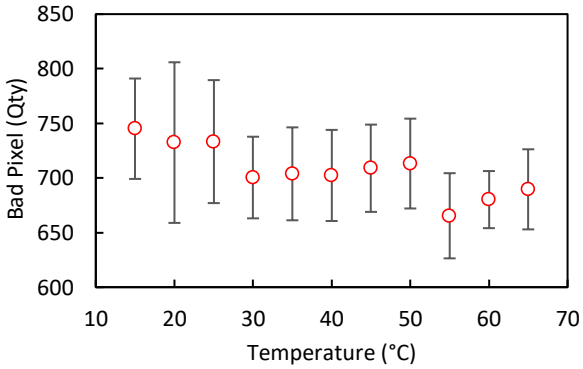

Fig. 4 - Bad pixel count, 3σ, given one reference temperature.

Another relevant aspect in the determination and location of these defective pixels was the lack of large amounts of pixels located in the central region of the matrix. Its vast majority is located at the edges. Fig. 5 shows the defective pixels location under two different conditions, in (a) obtained by the analysis of references C20H25 and (b) C55H65 largest and smallest defective pixels number respectively.

This method, definition, has generated values higher than the company evaluation (25 bad pixels), but the company has used a different criterion for identifying the bad pixels.

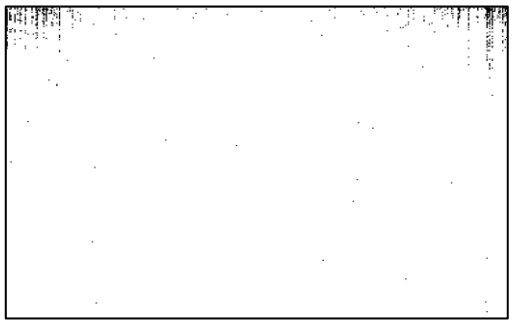

(a)

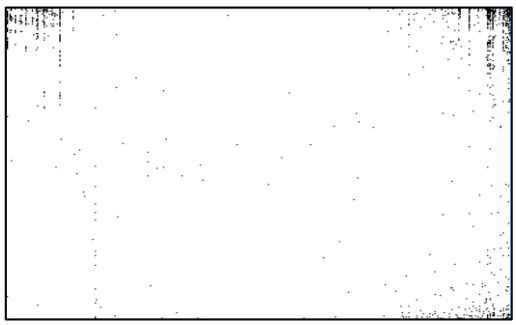

(b)

Fig. 5 - Bad pixels location with 3σ method. In (a) the best scene, C55H65, while in (b) the worst case, C20H25.

C. NUC Process

During NUC process, uniformity evaluation was the first analysis of all raw images obtained, from 15 °C to 65 °C, the temperature at which the FPA was submitted. The values of these uniformities were between 78-95% with their peak near 40 °C, Fig. 7 (a). It is important to note that such FPAs are produced for their best performance at temperatures approaching 36.5 °C, so this temperature was set for the sensors array, so, the uniformity is best when the blackbody is at a temperature close to the FPA temperature, meaning minimum liquid heat transfer.

With the non-uniformity correction, regardless of the temperature chosen as reference, there was a significant improvement in image uniformity. As expected, the highest uniformity was observed at the reference temperatures. Between and outside these points, there is a natural decrease. As the distance between the reference temperatures rises, the uniformity decreases between points and rises outside [3].

Fig. 6 show the improvement obtained when the reference temperatures for NUC were 15 and 20 °C (C15H20) and 25 and 60 °C (C25H60). However, the choice of the best temperatures for NUC required a mathematical rule. It was then determined the area between the curves before and after NUC, and this result was called efficiency. Given the result of uniformity without NUC, the maximum possible efficiency was 5.65 (area between the response curves and the 100% uniformity line).

Still as a tie-breaking criterion between the reference temperature conditions, the mean and the standard deviation of the uniformities obtained after NUC were calculated. Thus, if there was a tie in the area between the graphs, the highest mean would be chosen as the best point for the non-uniformity correction.

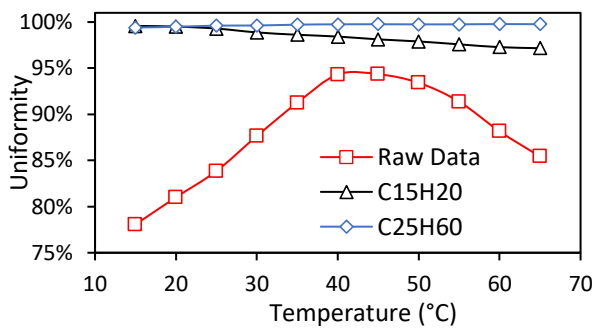

Fig. 6 - Uniformity as a function of blackbody temperature. In RAW images, and after NUC using reference C15H20 and C25H60.

The combinations with the highest efficiencies and highest uniformity averages are shown in Table 2. In this, we observe that the best options for NUC conjugate a temperature close to 30 °C for the lower and a temperature close to the limit of the range for the higher.

Table 2 - Best reference temperature combinations for FPA

Reference	ΔT (°C)	Efficiency	Avg. Uniformity	σ
C25H60	35	5.4854	99.67%	0.13%
C35H65	30	5.4829	99.67%	0.12%
C30H65	35	5.4801	99.66%	0.14%
C25H55	30	5.4796	99.66%	0.11%
C35H60	25	5.4782	99.66%	0.13%
C30H60	30	5.4777	99.66%	0.14%
C15H55	40	5.4765	99.66%	0.08%
C15H65	50	5.4763	99.67%	0.10%
C25H65	40	5.4763	99.67%	0.10%
C20H65	45	5.4762	99.66%	0.12%

On the other hand, the combinations having low ΔT, which are: C15H20, C60H65 and C20H25 showed the worst efficiency, Table 3. It is worth mentioning the tendency already cited by Holst, that there is a tendency to increase uniformity with the proximity of reference points. Nevertheless, if the calibration has to be done with low ΔT (5 °C), the results show that it will be a best choice temperature around 40 - 45 °C (C35H40 and C45H50) because these would be more efficient.

Table 3 - Worst reference temperature combinations

Reference	ΔT (°C)	Efficiency	Avg. Uniformity	σ
C15H20	5	4.8434	98.40%	0.86%
C60H65	5	5.0130	98.72%	0.94%
C20H25	5	5.0355	98.76%	0.68%
C25H30	5	5.0937	98.85%	0.61%
C55H60	5	5.1008	98.88%	0.85%
C50H55	5	5.1161	98.89%	0.88%
C40H45	5	5.1781	98.99%	0.65%
C30H35	5	5.1876	99.02%	0.52%
C35H40	5	5.2152	99.08%	0.46%
C45H50	5	5.2190	99.10%	0.65%

D. Responsivity

Following manufacturer standard, the reference points for the initial responsivity calculation were the temperatures 20 °C and 35 °C. It was observed that the responsivity in this case is far from specified. 11.2 mV/K was found, lower than the 12.8 mV/K indicated in its manual, an error of approximately 12%.

However, an analysis across the entire range of measures, Fig. 7, illustrates that the signal transfer function of the FPA can be even higher than specified, depending on the points chosen to the measurement, due to the nonlinearity of the curve.

The linear adjustment performed on the responsivity graph throughout the measurement range, since there were no signs of saturation in the FPA, gave us a SiTF average of 13.1 mV/K, higher than initially found when obtained through the points specified by the manufacturer. Table 3 shows the interval of greater linearity of the graph, its correlation coefficient and finally its SiTF.

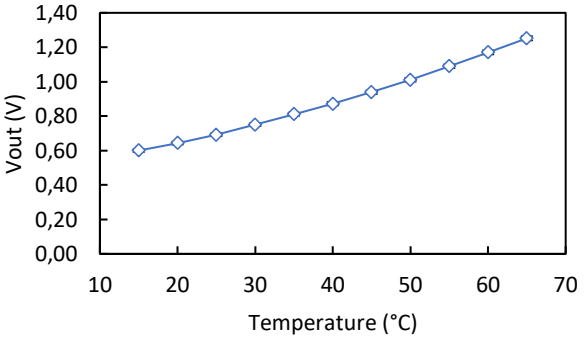

Fig. 7 - Responsivity curve for the test.

Table 3 - Linear region of the responsivity function

T_{min} T_{max}	Equation	R^2	SiTF (mV/K)
15-65	V_{out} (V) = 13.1x10^{-3} T + 0.370	0.992	13.1

Considering the different ways of measuring the SiTF, a point-to-point analysis of the line was performed to verify possible SiTF values for the FPA as a function of the reference temperature, fixing the "cold" as the lower or fixing the "hot" as the highest. The result generated the graph, on Fig. 8, where it is observed that the SiTF varied significantly, depending on the measurement points used. In this graph the lower and upper limits found for the SiTF are represented.

The upper curve is formed by the set of points where the hot reference temperature was 65 °C. In this curve a variation of 13.0 mV/K to 16.3 mV/K was observed. While the lower curve formed by the points at which the cold reference temperature (15°C) was chosen provided a response ranging from 8.6 to 13.0 mV/K.

It is emphasized that between the two curves there is a series of other combinations with intermediate values in the two illustrated curves.

Standard deviation in the responsivity measures was so small that the error bar is not visible in the graph.

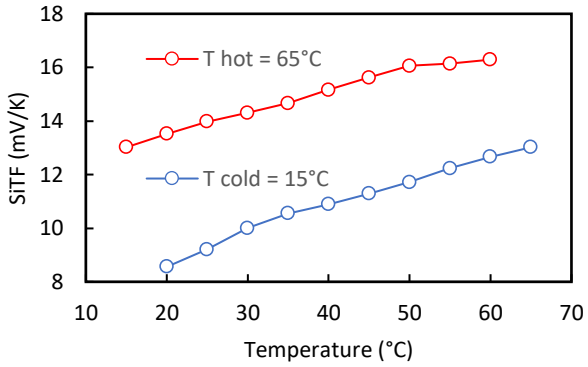

Fig. 8 - SiTF variation as a reference temperature function

E. NETD evaluation

The characterization through the direct reading of the ROIC, ended with the analysis of the noise present in the FPA and the analysis of the system's NETD.

The NETD was measured considering all temperature combinations as done during the NUC evaluation. The results were then consolidated in a graph, Fig. 9, in which the trend of the NETD as a function of the reference temperatures is present.

There is a decrease in the value of NETD with the increase of the reference temperatures. It is not surprising, since it scales inversely with SiTF, although it means that the noise has not change as much as the SiTF. The upper blue curve containing as lower reference temperature 15 °C and decays from over 110 mK to below 80 mK. Again, the choice of reference temperatures significantly influenced the results.

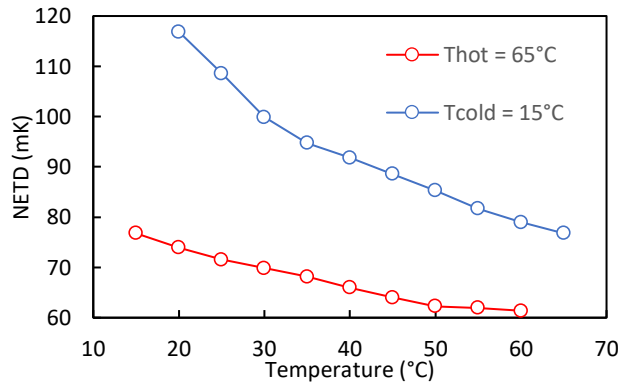

Fig. 9 - NETD variation as a reference temperature function.

IV. Conclusion

It was possible to show that the LWIR FPA calibration process is a function of the reference temperatures. As the hot reference temperature increase (higher than 55 °C) and the cold reference temperature keep close to 30 °C the uniformity obtained for this FPA has improved. On the other hand, for lower reference temperature, the noise increases and as a consequence of that, the uniformity is lower.

By choosing appropriate reference temperatures, a NETD lower than 70 mK @ f/1.4, a SiTF over than 13 mV/K and the uniformity higher than 99.67% could be obtained. These values are better than specified by the manufacturer.

Regarding the definition of bad pixel (sensitivity differs more than ± 3 standard deviation from the mean value) this was not effective, since the number of rejected pixels was dozens of times higher than the specified by the manufacturer. Other criteria will be analysed in future works.

A natural sequence of this paper is the study of defective pixel definitions and also modify parameters here fixed, such as Integration time, reference bias and FPA temperature.

References

[1] K. Chrzanowski, *Testing thermal imagers - Practical guidebook*. Warsaw, Poland: Military University of Technology, 2010.

[2] A. Kamoi, Y. Okamoto, and T. Ishii, "*Evaluation methods of NETD and MRTD for IR camera by using FLIR collimator*", Proc. SPIE 4360, Thermosense XXIII, (23 March 2001).

[3] G. C. Holst, *Testing and Evaluation of Infrared Imaging Systems*, 3th ed. Winter Park, FL: JCD Publishing and SPIE Press, 2008.

[4] G. C. Holst, *Electro-Optical Imaging System Performance*, 5th ed. Winter Park, FL: JCD Publishing and SPIE Press, 2008.

[5] A. Rogalski, "*Infrared detectors: status and trends*," *Prog. Quantum Electron.*, vol. 27, no. 2–3, pp. 59–210, 2003.

[6] K. Chrzanowski, J. Bareła, K. Firmanty, "*Testing of electro-optical imaging systems*" *Proc. SPIE - Int. Soc. Opt. Eng.*, vol. 5407, pp. 236–243, 2004.

[7] M. Krupiński, J. Bareła, K. Firmanty, M. Kastek, "*Test stand for non-uniformity correction of microbolometer focal plane arrays used in thermal cameras*" Proc. SPIE 8896, Electro-Optical and Infrared Systems: Technology and Applications X, 889611 (25 October 2013).

[8] M. Krupiński, J. Bareła, M. Kastek, K. Chmielewski, "*Test stand for determining parameters of microbolometer camera*" Proc. SPIE 9987, Electro-Optical and Infrared Systems: Technology and Applications XIII, 998712 (21 October 2016)

[9] J. M. L. Alonso, J. Alda, "*Bad pixel identification by means of principal components analysis*" *Opt. Eng.*, vol. 41, no. 9, pp. 2152–2157, 2002.

[10] J. M. L. Alonso, J. Alda , *"Principal component analysis of noise in an image-acquisition system: bad pixel extraction*" Photonics, Devices, Syst. II, no. July 2003, pp. 353–357, 2003.

[11] A. Daniels, *Field Guide to Infrared Systems, Detectors, and FPAs*, 2nd ed. Bellingham, Washington: SPIE Press, 2010.

[12] J. M. Lloyd, *Thermal Imaging Systems*. 1975.

[13] D. B. Beasley, *"Calibration and nonuniformity correction of MICOM's diode-laser-based infrared scene projector" Proc. SPIE*, vol. 3084, pp. 91–101, 1997.

[14] S.-C. Chao, H.-M. Huang, "*Variation of NETD caused by nonuniformity correction in thermal imager*" SPIE Conf. Infrared Syst. Des. Anal. Model. Test. IX, vol. 3377, no. August 1998, pp. 276–284, 1998.

[15] *Technical Data Specification* - UL 03 26 2 - 031 384x288 LWIR Uncooled Microbolometer.